

# Undetectable quantum transfer through a continuum

Jing Ping,<sup>1</sup> Yin Ye,<sup>1</sup> Xin-Qi Li,<sup>1,2</sup> YiJing Yan,<sup>3</sup> and Shmuel Gurvitz<sup>4</sup>

<sup>1</sup>State Key Laboratory for Superlattices and Microstructures, Institute of Semiconductors,  
Chinese Academy of Sciences, P.O. Box 912, Beijing 100083, China

<sup>2</sup>Department of Physics, Beijing Normal University, Beijing 100875, China

<sup>3</sup>Department of Chemistry, Hong Kong University of Science and Technology, Kowloon, Hong Kong

<sup>4</sup>Department of Particle Physics and Astrophysics,  
Weizmann Institute of Science, Rehovot 76100, Israel

(Dated: September 20, 2011)

We demonstrate that a quantum particle, initially prepared in a quantum well, can propagate through a reservoir with a continuous spectrum and reappear in a distant well without being registered in the reservoir. It is shown that such a passage through the reservoir takes place even if the latter is *continuously* monitored. We discuss a possible realization of such a teleportation phenomenon in experiments involving photon transfer between two optical cavities by using the available state-of-the-art technology.

PACS numbers: 03.65.Yz, 42.50.-p, 73.23.-b

## I. INTRODUCTION

It is well-known that quantum motion of a wave-packet is a result of quantum interference between the wave-packet's components of different energies. Despite its interference feature, the quantum motion of a wave packet in a continuum is similar to a free motion of a classical particle. However, in some cases, the quantum motion through a continuum can be drastically different from its classical counterpart due to quantum interference on large scales.

Consider for instance a quantum well coupled to an infinite reservoir. Then a particle initially localized inside the well would eventually disappear in the reservoir. This is not surprising, since number of states in the reservoir is infinitely larger than that in the quantum well. However, if an another distant well is coupled to the same reservoir, as shown in Fig. 1, the situation can be quite different. It was demonstrated in Refs. [1,2] that the particle does not always decay to the reservoir at  $t \rightarrow \infty$ , but it can be found in the second well with a *finite* probability (1/4 for a symmetric case), provided that the energy levels of both wells are aligned, i.e.  $E_1 = E_2$  in Fig. 1. One can expect that such a motion between distant localized states, through the continuum, would display interference effects on large distances and therefore would be very different from the classical motion. Thus, it is desirable to investigate this process in more details.

Let us assume that we *continuously* monitor the reservoir, Fig. 1, and select only the events in which no particle is registered in the reservoir at any time ("null-result" continuous measurement). The question is whether the particle can be found in the right well, which was initially unoccupied? In fact, the unitary Schrödinger evolution, considered in<sup>1,2</sup>, does not tell us what would happen with the system, which is continuously measured. We can only anticipate that even the null-result measurement would strongly affect its motion<sup>3,4</sup>. Since in our case two distant wells are not directly coupled but only through the con-

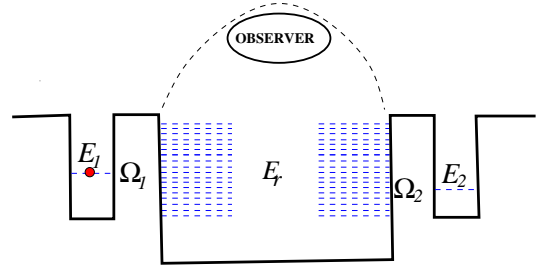


FIG. 1: (color online) A particle in two quantum wells separated by a reservoir, which is continuously monitored.  $E_{1,2}$  and  $E_r$  are the energy levels of the wells and of the reservoir, and  $\Omega_{1(2)}$  denote the couplings between the wells and the reservoir.

tinuum, Fig. 1, one would expect that in all events when the particle does not appears in the reservoir, it would remain in the left well and thus would never appear in the right well.

Surprisingly enough, this assertion is not correct. We demonstrate in this paper that the particle can be found in the right well with a finite probability, without being registered in the reservoir. Moreover, it appears that such an undetectable ("teleportation") phenomenon<sup>5</sup> characterizes all transitions through the continuum between two distant isolated states. For instance, if the particle is detected in the reservoir, it would not appear in the right well anymore.

The paper is organized as follows. In Sec. IIA we describe a single particle motion between two distant quantum wells, separated by the reservoir without any measurement of the particle in the reservoir<sup>2</sup>. A role of a bound state embedded in the continuum is elaborated. In Sec. IIB we cast the master equations describing the unitary evolution of the system in a Lindblad form. In Sect. IIC we investigate continuous monitoring of the particle motion in the reservoir by applying the quantum trajectory approach. Numerical results are presented in

Sec. IID that illustrate main features of the undetectable quantum transfer between distant wells. Sec. III suggests a possible realization of such a teleportation phenomenon in optical experiments. Finally, in Sec. IV we briefly summarize the work.

## II. QUANTUM PARTICLE IN TWO DISTANT WELLS SEPARATED BY A CONTINUUM

### A. Bound state embedded in the continuum

Consider two distant quantum wells coupled to a common reservoir with a single particle places inside one of the wells, Fig. 1. This particle can be either a boson or a fermion. For a simplicity, we assume that each of the wells contains only one level ( $E_1$  and  $E_2$ ). The reservoir states,  $E_r$ , are very dense (continuum) with a density of states  $\rho$ . The system is described by the following tunneling Hamiltonian:

$$H = E_1 |1\rangle\langle 1| + E_2 |2\rangle\langle 2| + \sum_r E_r |r\rangle\langle r| + \sum_r (\Omega_1 |1\rangle\langle r| + \Omega_2 |2\rangle\langle r| + H.c.), \quad (1)$$

where  $|1\rangle$ ,  $|2\rangle$  are *localized* states of the quantum wells and  $|r\rangle$  denote *extended* states of the reservoir. In the absence of a magnetic field the couplings between the reservoir and the wells,  $\Omega_1$  and  $\Omega_2$ , are real, but they can be of opposite sign, depending on the relative parity (number of nodes) of the states  $|1\rangle$ ,  $|2\rangle$  in the quantum wells<sup>7</sup>.

The wave function of a quantum particle in this system can be written in the most general way as

$$|\Psi(t)\rangle = b_1(t) |1\rangle + b_2(t) |2\rangle + \sum_r b_r(t) |r\rangle, \quad (2)$$

where  $b_{1,2}(t)$  and  $b_r(t)$  are the probability amplitudes of finding the electron in the wells or in the reservoir, respectively. These amplitudes are obtained from the time-dependent Schrödinger equation

$$i \partial_t |\Psi(t)\rangle = H |\Psi(t)\rangle, \quad (3)$$

where the Hamiltonian  $H$  is given by Eq. (1). One easily finds that in the case of aligned levels,  $E_1 = E_2$ , the localized state

$$|1'\rangle = \frac{1}{\sqrt{\Omega_1^2 + \Omega_2^2}} (\Omega_2 |1\rangle - \Omega_1 |2\rangle), \quad (4)$$

is an eigenstate of the Hamiltonian (1). Indeed

$$H |1'\rangle = \frac{1}{\sqrt{\Omega_1^2 + \Omega_2^2}} (E_1 \Omega_2 |1\rangle - E_2 \Omega_1 |2\rangle) = E_1 |1'\rangle \quad (5)$$

The state  $|1'\rangle$  reveals striking example of a bound (localized) state embedded in the continuum<sup>8</sup>. This state is

not hybridized with the reservoir states and therefore is similar to a “dark” state in quantum optics. In contrast, the localized state  $|2'\rangle$ , orthogonal to  $|1'\rangle$

$$|2'\rangle = \frac{1}{\sqrt{\Omega_1^2 + \Omega_2^2}} (\Omega_1 |1\rangle + \Omega_2 |2\rangle), \quad (6)$$

is not an eigenstate of the Hamiltonian (1). It decays to the reservoir as  $e^{-(\Gamma_1 + \Gamma_2)t}$ , where  $\Gamma_{1,2} = 2\pi\rho\Omega_{1,2}^2$  is the width of the levels  $E_{1,2}$  (see Ref. 2). Therefore, any initial state  $|\Phi_0\rangle$  inside the wells, which can be represented as a linear superposition of the states  $|1'\rangle$  and  $|2'\rangle$ ,

$$|\Phi_0\rangle = \alpha_1 |1'\rangle + \alpha_2 |2'\rangle, \quad (7)$$

would not totally decays to the continuous states of the reservoir in the limit  $t \rightarrow \infty$ , but survives in the state  $|1'\rangle$  with the probability  $|\alpha_1|^2 = |\langle 1' | \Phi_0 \rangle|^2$ . For instance if the particle is initially localized in the left well of Fig. 1,  $|\Phi_0\rangle = |1\rangle$ , it can be found at  $t \rightarrow \infty$  in the right well with a *finite* probability  $\Omega_1^2 \Omega_2^2 / (\Omega_1^2 + \Omega_2^2)^2$ .

If, however, the levels are not aligned,  $E_1 - E_2 = \varepsilon \neq 0$ , there are no localized eigenstates in the continuous spectrum of the Hamiltonian (1). As a result, a particle localized initially inside the wells would always decay to the continuum at  $t \rightarrow \infty$ .

### B. Lindblad master equations

In order to determine the time-evolution of a prepared state localized in the wells, one needs to solve the time-dependent Schrödinger equation (3) for the wave function  $|\Psi(t)\rangle$ , Eq. (2). It would be useful, however to use the density-matrix  $\sigma_{jj'}(t)$  with  $j, j' = \{1, 2\}$ , instead of the wave function, defined as

$$\sigma_{11}(t) = |b_1(t)|^2, \quad \sigma_{22}(t) = |b_2(t)|^2, \quad \sigma_{12}(t) = b_1(t)b_2^*(t). \quad (8)$$

It was shown in Ref. [2] that Eq. (3) can be reduced to the master equations for this density matrix by tracing the reservoir states in the equation of motion. One finds

$$\dot{\sigma}_{11}(t) = -\Gamma_1 \sigma_{11}(t) - \pi\rho \Omega_1 \Omega_2 [\sigma_{12}(t) + \sigma_{21}(t)] \quad (9a)$$

$$\dot{\sigma}_{22}(t) = -\Gamma_2 \sigma_{22}(t) - \pi\rho \Omega_1 \Omega_2 [\sigma_{12}(t) + \sigma_{21}(t)] \quad (9b)$$

$$\dot{\sigma}_{12}(t) = i(E_2 - E_1)\sigma_{12}(t) - \pi\rho \Omega_1 \Omega_2 [\sigma_{11}(t) + \sigma_{22}(t)] - \frac{\Gamma_1 + \Gamma_2}{2} \sigma_{12}(t). \quad (9c)$$

Equations (9) can be rewritten as the Lindblad equation

$$\dot{\sigma} = -i[H_S, \sigma] + \Gamma_1 \mathcal{D}[a_1 + \chi a_2] \sigma. \quad (10)$$

Here  $H_S = E_1 |1\rangle\langle 1| + E_2 |2\rangle\langle 2|$ ,  $\chi = \Omega_2/\Omega_1$  and  $a_1 = |0\rangle\langle 1|$ ,  $a_2 = |0\rangle\langle 2|$ , where the state  $|0\rangle$  corresponds to empty quantum wells with the particle is inside the

reservoir, so the corresponding density-matrix element is  $\sigma_{00}(t) = 1 - \sigma_{11}(t) - \sigma_{22}(t)$ . The Lindblad super-operator is defined through

$$\mathcal{D}[a]\sigma = a\sigma a^\dagger - \frac{1}{2}\{a^\dagger a, \sigma\}, \quad (11)$$

where  $a \equiv a_1 + \chi a_2$ .

Equations (9) (or (10)) can be solved analytically. For instance, for the symmetric case,  $\Gamma_1 = \Gamma_2 = \Gamma$  and for the initial conditions corresponding to the particle in the left well, the probability of finding the particle inside the left and the right well are<sup>1,2</sup>

$$\sigma_{11}(t) = \frac{\Gamma^2 \cosh^2(\omega t/2) - \varepsilon^2}{\omega^2} e^{-\Gamma t}, \quad (12a)$$

$$\sigma_{22}(t) = \frac{\Gamma^2 \sinh^2(\omega t/2)}{\omega^2} e^{-\Gamma t}, \quad (12b)$$

where  $\omega = \sqrt{\Gamma^2 - \varepsilon^2}$ .

It follows from these equations that for aligned levels ( $\varepsilon = 0$ ) probability of finding the particle inside the wells in the asymptotic limit,  $\sigma_{22}(t \rightarrow \infty) = 1/4$ . If, however,  $\varepsilon \neq 0$ , one finds  $\sigma_{22}(t \rightarrow \infty) = 0$ . Nevertheless for small displacement  $\varepsilon \lesssim \Gamma$ , the particle spends long time ( $\sim \Gamma/\varepsilon^2$ ) inside the right well before it decays to the reservoir<sup>2</sup>. Thus the effect is still exists, even so the condition of aligned levels is not precisely fulfilled.

### C. Particle transfer through the reservoir under continuous null-result measurement

It is natural to assume that a particle, initially localized in the left well, arrives to the right well from the reservoir. In particular, this is expected from the Hamiltonian (1) which couples two wells only through the reservoir. In order to check this point, we have to monitor the reservoir continuously on the time-interval  $(0, t)$ . For this reason we insert the detector (“observer”), Fig. 1, that registers the particle in the reservoir at each time-intervals  $dt = t/n$ , choosing only the null-result measurements (no particle is detected in the reservoir). Then in the limit of *continuous* null-result measurement,  $n \rightarrow \infty$ , one would anticipate that the particle remains locked in the left well and therefore would never appear in the right well.

In fact there exists a well-developed theory of continuous quantum measurement, describing the measurement-results conditioned state evolution. The resulting evolution is governed by the quantum trajectory equation<sup>9</sup>. In our case this equation reads:

$$d\rho = dN(t) \mathcal{G}[a]\rho - dt \mathcal{H}[iH_S + \Gamma_1 a^\dagger a/2]\rho. \quad (13)$$

Here we use  $\rho \equiv \rho(t)$  to denote the conditional density-matrix, rather than unconditional one,  $\sigma(t)$  in Eqs. (9). The super-operators are defined as<sup>9</sup>  $\mathcal{G}[a]\rho = a\rho a^\dagger / \text{Tr}[a\rho a^\dagger] - \rho$ , and  $\mathcal{H}[x]\rho = x\rho + \rho x^\dagger - \langle x + x^\dagger \rangle \rho$

where  $\langle \dots \rangle \equiv \text{Tr}[(\dots)\rho]$ .  $dN(t) = 0$  or 1, being the measurement record of particle number detected in the reservoir during the time interval  $(t, t + dt)$ .

The above Eq. (13) is associated with an evolution based on a given measurement record. Consider the evolution under condition of the null-result measurement. For continuous measurement it corresponds to  $dN(t) = 0$  in Eq. (13). Conditioned on this requirement, the state evolution is given by

$$\begin{aligned} \dot{\rho} &= -\mathcal{H}[iH_S + \Gamma_1 a^\dagger a/2]\rho \\ &= -i[H_S, \rho] + \Gamma_1 \left( \text{Tr}[a^\dagger a \rho] \rho - \frac{1}{2}\{a^\dagger a, \rho\} \right). \end{aligned} \quad (14)$$

This is actually a *nonlinear* equation. Nevertheless its solution can be written in a simple way by introducing an effective evolution operator  $\mathcal{U}_{\text{eff}}(t, 0)$ , as follows

$$\rho(t) = \mathcal{U}_{\text{eff}}(t, 0) \rho(0) \mathcal{U}_{\text{eff}}^\dagger(t, 0) / \|\cdot\|, \quad (15)$$

where  $\mathcal{U}_{\text{eff}}(t, 0) = \exp[-i(H_S - i\frac{\Gamma_1}{2}a^\dagger a)t]$ . Here  $\|\cdot\|$  denotes the trace of the numerator that normalizes the state, reflecting a non-unitarity of  $\mathcal{U}_{\text{eff}}(t, 0)$ .

Equation (15) can be easily solved in the basis of the states  $|1'\rangle$  and  $|2'\rangle$ , Eqs. (4), (6). The solution has a particularly simple form for the symmetric case:  $\Gamma_1 = \Gamma_2 = \Gamma$ . One finds from Eq. (15) that

$$\rho_{11}(t) = \frac{\cosh \omega t + 1 - 2\varepsilon^2/\Gamma^2}{2(\cosh \omega t - \varepsilon^2/\Gamma^2)} \quad (16a)$$

$$\rho_{22}(t) = \frac{\cosh \omega t - 1}{2(\cosh \omega t - \varepsilon^2/\Gamma^2)} \quad (16b)$$

(c.f. with Eqs. (12)). Thus, contrary to the expectations, the particle is not locked in the left well under the *continuous* null-result measurement condition in the reservoir. It can be found in the right well with a *finite* probability. This implies that the particle jumps directly to the right well without passing the reservoir, although the wells can be largely separated in space. Since such a jump cannot take place via the reservoir states, it proceeds through the bound state  $|1'\rangle$ , Eq. (4), embedded in the continuum. This state is a part of the total Hamiltonian spectrum. However it does not belong to the reservoir states and therefore the transport via this state cannot be detected by continuously monitoring the reservoir.

Comparing  $\rho_{11}(t)$  and  $\rho_{22}(t)$  with  $\sigma_{11}(t)$  and  $\sigma_{22}(t)$ , given by Eqs. (12), one finds that the both quantities are quite different. For instance,  $\rho_{11} = \rho_{22} = 1/2$  in the asymptotic limit ( $t \rightarrow \infty$ ) for any  $\varepsilon$ , whereas in the same limit  $\sigma_{11} = \sigma_{22} = 1/4$  for  $\varepsilon = 0$  and  $\sigma_{11} = \sigma_{22} = 0$  for any  $\varepsilon \neq 0$ . This is not surprising since  $\rho(t)$  is the conditional probability, subjected to the requirement that only events with no particle in the reservoir are counted. On the other hand,  $\sigma(t)$  is the unconditional density matrix describing all events, including those when the particle disappears in the reservoir. As a result the probability of finding the particle inside the

wells,  $P_0(t) = \sigma_{11}(t) + \sigma_{22}(t)$ , is smaller than one. Indeed,  $P_0(t \rightarrow \infty) = 1/2$ , Eq. (12). The conditional density matrix,  $\sigma_{jj'}^{(c)}(t)$ , for finding the particle in each of the wells at time  $t$  is therefore

$$\sigma_{jj'}^{(c)}(t) = \frac{\sigma_{jj'}(t)}{\text{Tr}[\sigma(t)]} = \frac{\sigma_{jj'}(t)}{P_0(t)}, \quad \text{for } j, j' = \{1, 2\}. \quad (17)$$

In contrast with  $\rho(t)$  which implies that no particle is found in the reservoir on a *whole* time-interval time  $(0, t)$ , the conditional probability  $\sigma_{jj'}^{(c)}(t)$ , given by Eqs. (9), (10), is much less restrictive. It only implies that no particle in the reservoir is found at time  $t$ . However at any other time  $t'$  inside the interval  $(0, t)$ , the particle can appear in the reservoir. As a result, one would expect that the conditional probability  $\sigma_{jj'}^{(c)}(t)$ , obtained from the Schrödinger evolution would exceed  $\rho(t)$  obtained from the quantum trajectory equation (14). However, it follows from Eqs. (12) and (16) that

$$\rho_{jj'}(t) = \sigma_{jj'}^{(c)}(t). \quad (18)$$

Although the l.h.s. and r.h.s. of Eq. (18) are related to different systems (with and without the detector), this equality implies a striking picture: in *all* transitions between the two distant wells (measured or not), it looks like that the particle is not appeared in the reservoir.

In fact, Eq. (18) can be obtained from rather general arguments. Let us consider Eqs. (3) describing the evolution of the total wave function,  $|\Psi(t)\rangle$ . The null-result measurement in the reservoir implies that the particle is inside the well. Therefore the wave function is projected to the subspace of the two wells,  $|\Psi(t)\rangle \rightarrow \mathcal{P}_2|\Psi(t)\rangle$ , where

$$\mathcal{P}_2 = \frac{1}{\sqrt{\mathcal{N}}}(|1\rangle\langle 1| + |2\rangle\langle 2|), \quad (19)$$

is the projector on this subspace and  $\mathcal{N}$  is a normalization factor. It is very crucial for our arguments that the Schrödinger equation (3) can be reduced to the system of closed linear equations (9) for the reduced density matrix  $\sigma(t)$  in the subspace of the two wells. In this subspace the projector  $\mathcal{P}_2$ , Eq. (19), is proportional to the *unit* matrix, up to the overall normalization. Therefore any repeated  $n$  null-result measurements correspond to  $n$  subsequent projections of the density matrix,  $\mathcal{P}_2\sigma(t)\mathcal{P}_2$ , affecting its time development given by Eqs. (9), by the normalization factor only. As a result, the conditional density matrix, subjected to  $n$  null-result measurement,  $\rho(t)$  is given by

$$\rho(t) = \frac{1}{\mathcal{N}_1} \cdots \frac{1}{\mathcal{N}_n} \sigma(t) = \frac{\sigma(t)}{\text{Tr}[\sigma(t)]}. \quad (20)$$

which coincides with Eq. (18).

#### D. Numerical analysis

Consider first the conditional density matrix  $\rho(t)$  for the case of the same level-widths  $\Gamma_1 = \Gamma_2 = \Gamma$ . The

corresponding couplings  $\Omega_{1,2}$ , however, can be of opposite sign,  $\Omega_1 = \pm\Omega_2$ , depending on the relative parity of the well states,  $\eta = \Omega_1/\Omega_2 = \pm 1$ . Conditional probabilities for occupation of the left and right wells,  $\rho_{11}(t)$  and  $\rho_{22}(t)$ , Eqs. (16), are displayed in Fig. 2 for the initial condition corresponding to the occupied left well. Both are independent of  $\eta$ . The latter affects only the off-diagonal term, as illustrated in the inset of Fig. 2. The solid curves correspond to aligned levels,  $\epsilon = 0$  and the dashed curves to displaced levels,  $\epsilon \neq 0$ . In both cases the occupation probabilities reach the same asymptotic limit, and the effect of level displacement is unessential. This is drastically different from the asymptotic behavior of the unconditional density matrix,  $\sigma(t)$ , Eq. (12), that vanishes in the asymptotic limit for any finite  $\epsilon$ , no matter how small it is.

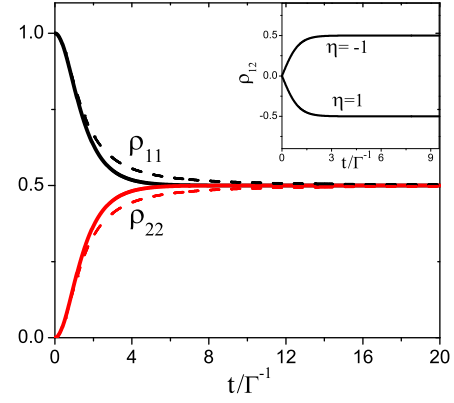


FIG. 2: (color online) Occupation of the wells, conditioned on the null result of continuous measurement in the reservoir for  $\Gamma_1 = \Gamma_2 = \Gamma$ . The solid lines correspond to  $E_1 = E_2$ , while the dashed lines to  $E_1 - E_2 = \pm 0.5\Gamma$ . Inset: the off-diagonal element of the density matrix for  $\eta = \pm 1$  and  $E_1 = E_2$ .

The reason for such a different behavior is quite clear. Indeed, probability of an event where the particle is *not found* inside the reservoir becomes very small for  $\epsilon \neq 0$  and large  $t$ , since the unconditional density matrix,  $\sigma(t)$  vanishes at  $t \rightarrow \infty$ . However, if such an event takes place at time  $t$ , it implies that the particle stays inside the dots in the time interval  $(t, t + \Delta t)$  with probability one for  $\Delta t \rightarrow 0$ . Therefore the *conditional probability* of finding the particle in each dot is not vanishes at  $t \rightarrow \infty$  for  $\epsilon \neq 0$ . It reaches the value of 1/2 for symmetric dots, as shown in Fig. 2.

The conditional occupation probabilities in the steady state,  $\bar{\rho} = \rho(t \rightarrow \infty)$ , as a function of the coupling asymmetry  $\chi = \Omega_2/\Omega_1$ , are shown in Fig. 3 for aligned and misaligned levels. As in Fig. 2 the level misalignment ( $\epsilon$ ) have minor effects on the stationary occupation probabilities, in contrast with the unconditional probabilities<sup>2</sup>. However, similar to unconditional probabilities, the asymmetry of coupling between the con-

tinuum and the well strongly affects both the transient process and the stationary state in an unexpected way. Indeed the unconditional probability of transfer from the left to the right well, Eqs. (12), increases, when the coupling of the right well with the reservoir,  $\Omega_2$ , decreases! This peculiar behavior has been explained in Ref. 2 in terms of quantum interference at large scale. In the case of conditional probabilities the same behavior of transition probabilities, displayed in Fig. 3, can be understood by an information-theoretic interpretation. Consider, for instance,  $\Gamma_2 < \Gamma_1$ , corresponding to  $\Omega_2/\Omega_1 < 1$ . The null-result of measurement in the reservoir indicates that probability of finding the electron in the right dot is larger than that in the left dot. In the opposite case,  $\Gamma_1 < \Gamma_2$ , the electron is more likely to be found in the left dot, conditioned on the same null result of measurement.

We also like to mention that the conditional probability  $\bar{\rho}$  at  $\chi = 0$  implies the following order of limits:  $\bar{\rho} = \lim_{\chi \rightarrow 0} \lim_{t \rightarrow \infty} \bar{\rho}$ . The inverse order would result in  $\bar{\rho}_{11} = 1$  and  $\bar{\rho}_{22} = 1$  at  $\chi = 0$ . Consequently,  $\bar{\rho}$  displays a nonanalytic behavior at  $\chi = \Omega_2/\Omega_1 = 0$ , as shown in Fig. 3. Note also that one cannot change a sign of  $\chi$  by a modulation of the barrier height. One needs to change the quantum well parameters in such a way that the corresponding wave function obtains an additional node<sup>7</sup>.

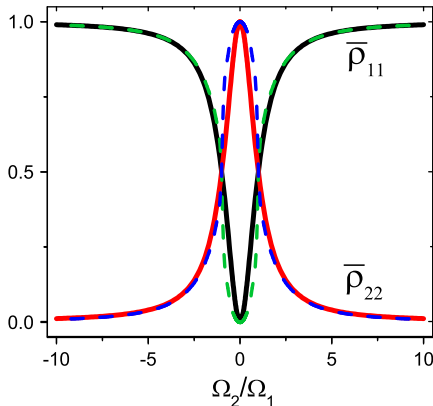


FIG. 3: (color online) Steady-state occupation probabilities as a function of the coupling asymmetry. Similar to Fig. 2, the solid curves correspond to  $E_1 = E_2$ , while the dashed curves correspond to  $E_1 - E_2 = \pm 0.5\Gamma$ .

As a final remark to the phenomenon of undetectable quantum transfer through continuum discussed in this section, it looks like that such a state evolution dramatically differs from the Zeno effect<sup>4</sup>. Indeed, the latter would attempt to freeze the particle in the initial state. The basic reason for this difference is that our observation only registers a non-appearance of the particle in the reservoir. However, it does not provide an information in which of the two wells the particle is. As a result, such a measurement cannot freeze the particle in a particular well.

### III. PHOTON TELEPORTATION BETWEEN TWO OPTICAL CAVITIES

The system of two distant quantum wells, discussed in the previous section represents a generic setup, which can be realized in different experiments. In this section we consider its possible realization in the optical system, schematically shown in Fig. 4. It represents two optical cavities separated away by free space (vacuum). Each cavity contains a two-level atom in it. The system is well described by the Hamiltonian<sup>10</sup>:

$$H_S = \sum_{j=1,2} \left[ \omega_j a_j^\dagger a_j + \frac{\Delta_j}{2} \sigma_j^z + g_j (\sigma_j^+ a_j + \sigma_j^- a_j^\dagger) \right], \quad (21)$$

where the first term describes the cavity photons, the second term is related to the atoms, and the third one to their couplings. Each cavity is taken to be one-sided coupled to the vacuum reservoir, where the cavity photon can leak out. For the sake of completeness, one may include in this equation the atom spontaneous emissions in the cavities. Owing to the Purcell effect, however, they should be very weak and therefore will be neglected in this work. The coupling is described by a tunneling Hamiltonian

$$H' = \sum_k [V_k (a_1 + a_2) b_k^\dagger + \text{h.c.}], \quad (22)$$

which would lead to a Lindblad master equation, Eq. (10) for the reduced state of the atoms plus the cavity photons:  $\dot{\rho} = -i[H_S, \rho] + \kappa \mathcal{D}[a]\rho$ . Here, again, we use the notation  $a = a_1 + a_2$ , while  $\kappa = 2\pi|V_k|^2 \varrho_{\text{ph}}$  is the leakage rate of the cavity photon, where  $\varrho_{\text{ph}}$  is the density of photon states in the vacuum.

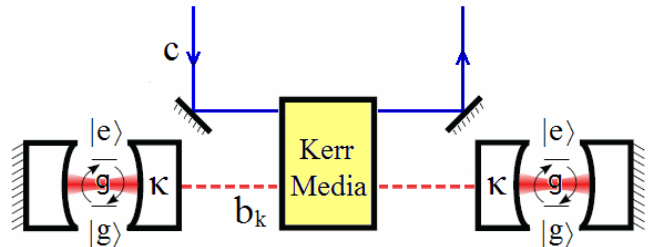


FIG. 4: (color online) Two optical cavities, each containing a two-level atom, are separated by the vacuum reservoir. The photon transfer between the two cavities, associated with the atomic excitation can be measured using quantum jumps technique. The photon emitted into the reservoir can be detected in a non-demolition way by using the optical-nonlinearity-induced interaction between photons in the Kerr medium, as explained in the text.

We assume that the atom in the left cavity is initially prepared by a pulsed laser driving in the excited state  $|e\rangle$  and the atom in the right cavity remains in the ground



state  $|g\rangle$ , meanwhile the both cavities are empty (without photon). Due to coupling between the atom and the cavity field, the atom (in the left cavity) would experience Rabi transition from  $|e\rangle$  to  $|g\rangle$ , generating a photon in the cavity. Mediated by the vacuum reservoir, this photon can be transferred to the right cavity, causing further atomic excitation (from  $|g\rangle$  to  $|e\rangle$ ) that can be measured using the quantum jumps technique with unit efficiency<sup>11</sup>.

### A. Quantum Non-Demolition Measurement in the Reservoir

The present optical setup allows for a quantum non-demolition (QND) measurement for the photon emitted in the reservoir. Based on existing technology, this can be realized with the help of a nonlinear Kerr medium, which can mediate an effective interaction between photons. For the setup depicted in Fig. 4, this type of interaction can be expressed by  $H_{\text{meas}} = -\chi b^\dagger b c^\dagger c$ , where  $c$  and  $c^\dagger$  are the annihilation and creation operators of the probing light that is prepared in a single-mode coherent state  $|\alpha\rangle$ , and  $b^\dagger b \equiv \sum_k b_k^\dagger b_k$  is the number operator of photons in the reservoir. The basic idea of the measurement is simply as follows. If a photon is emitted from one of the cavities, it will pass through the Kerr medium with some transmission time ( $\tau$ ), and cause a phase shift of the probing light ( $|\alpha\rangle \rightarrow |\alpha e^{i\chi\tau}\rangle$ ). Using the well-developed interferometry technique, such as the homodyne (or heterodyne) measurement<sup>9</sup> or the Mach-Zender interferometer<sup>12</sup>, this phase shift, can be readily read out with extremely high accuracy<sup>13</sup>.

### B. Results and Discussions

In Fig. 5 we illustrate the dynamics of photon transfer between the two cavities subjected to the continuous *null result* measurements. It looks different from Fig. 2, corresponding to continuous measurement for a generic setup in Fig. 1. The reason is that in each optical cavity the system undergoes the Rabi oscillations. Besides that the basic physics of photon transitions between two cavities remains the same.

Specifically, we consider a symmetric setup with identical cavities and atoms:  $\omega_1 = \omega_2$ ,  $\Delta_1 = \Delta_2$ , and  $g_1 = g_2 = g$  in Eqs. (21), (22). In our numerical simulations, the following five states are involved into the dynamics:  $|1\rangle = |0, e\rangle_1 \otimes |0, g\rangle_2$ ,  $|2\rangle = |1, g\rangle_1 \otimes |0, g\rangle_2$ ,  $|3\rangle = |0, g\rangle_1 \otimes |1, g\rangle_2$ ,  $|4\rangle = |0, g\rangle_1 \otimes |0, e\rangle_2$ , and  $|5\rangle = |0, g\rangle_1 \otimes |0, g\rangle_2$ . Here, in the notation  $|1(0), g(e)\rangle_j$ , “1(0)” stands for the photon number and “g(e)” for the atom state, while the subscript “j=1,2” labels the left and right cavities. The probabilities of finding the system in these states are therefore  $\rho_{ii}(t) = |\langle \Psi(t) | i \rangle|^2$ .

These probabilities are displayed in Fig. 5(a) and (b) for  $g = 0.2\kappa$  and  $g = 2.0\kappa$ , respectively, correspond-

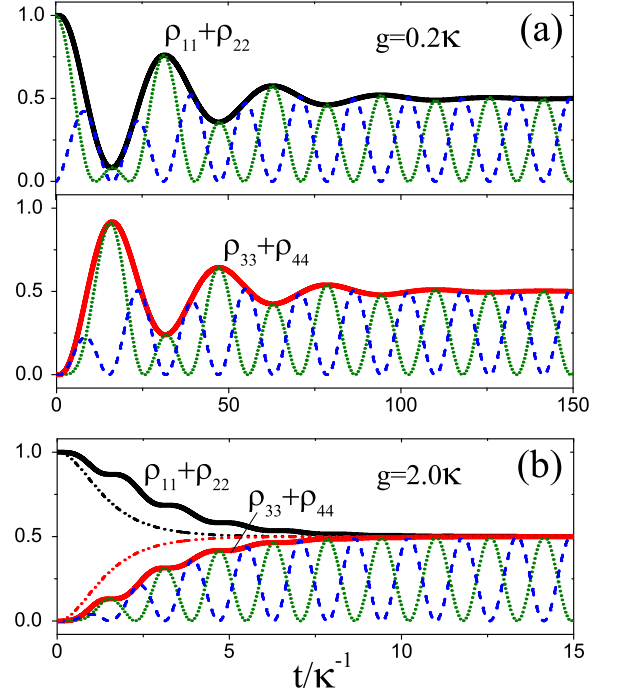


FIG. 5: (color online) Quantum transfer dynamics conditioned on the null-result measurement for slow and fast Rabi oscillations: (a)  $g = 0.2\kappa$  and (b)  $g = 2\kappa$ . The solid black (red) lines stand for the total occupation probabilities,  $\rho_{L(R)}(t)$  for the left (right) well. The partial occupation probabilities are shown by the green dotted for  $\rho_{11}$  and  $\rho_{44}$ , and by the blue dashed for  $\rho_{22}$  and  $\rho_{33}$ . Dot-dashed lines (black and red) in (b) show the particle (photon) occupation probabilities for the left (right) well, as given by the setup in Fig. 1, Eqs. (16).

ing to slow and fast Rabi-transitions inside the cavities. The green dotted lines show  $\rho_{11}(t)$  and  $\rho_{44}(t)$  and the blue dashed lines show  $\rho_{22}(t)$  and  $\rho_{33}(t)$ , respectively. The solid black and red lines in Fig. 5 show total occupation probabilities of the left and the right cavities,  $\rho_L(t) = \rho_{11}(t) + \rho_{22}(t)$  and  $\rho_R(t) = \rho_{33}(t) + \rho_{44}(t)$ , corresponding to atom is in the excited state or in the ground state accompanied by a photon. These total probabilities display the undetectable photon transfer (teleportation) between the cavities, modulated by the Rabi oscillations.

One finds from Fig. 5(a) that the frequency of these modulations is a half of the Rabi frequency. It can be understood in the following way. Obviously, photon transfer can take place after it is emitted by the atom in the left cavity. Then its transfer to the right cavity leads to its absorption by the atom and the following re-emission through the Rabi cycle. Next the photon is transferred back to the left cavity with its absorption by the atom. The total cycle therefore consists of two Rabi cycles.

In the case of fast Rabi oscillation, probability of the photon transfer during one Rabi cycle is not sufficiently large to produce oscillations in the total occupation probabilities,  $\rho_{L,R}(t)$ , as those in Fig. 5(a) for slow Rabi tran-

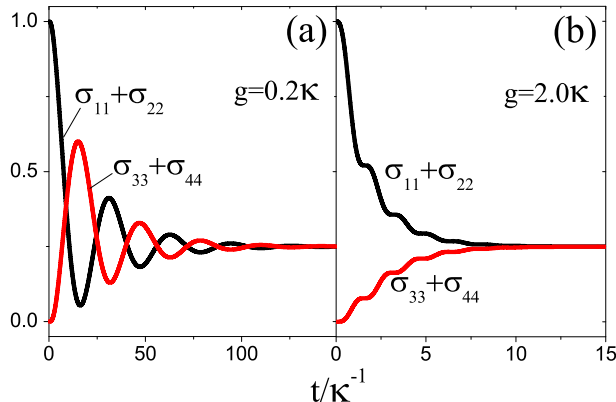


FIG. 6: (color online) The same as in Fig. 5 but for unconditional probabilities,  $\sigma(t)$  (without photon detection by the Kerr media in Fig. 4).

sitions. As a result,  $\rho_{L,R}(t)$  display a number of plateaus towards the steady state, Fig. 5(b), replacing the damped oscillations in Fig. 5(a).

For a comparison, we present in Fig. 5(b) the photon occupation probabilities for the setup in Fig. 1, Eqs. (16). These probabilities for the left (right) cavities are shown by the black (red) dot-dashed lines. One finds that the Rabi transitions inside the cavities delay the relaxation time to the steady state, which increases with decrease of the Rabi frequency, Figs. 5 (a,b). This phenomenon can be easily understood by taken into account that an increase of the Rabi frequency decreases fluctuations in the total occupation of each of the cavities.

Finally, we show in Fig. 6 the unconditional probabilities for the photon-transfer dynamics (with no photon detection in the vacuum reservoir). One finds that the basic dynamics for the unconditional probabilities,  $\sigma_{ii}(t)$ , modulated by the Rabi oscillations are similar to that discussed above.

#### IV. SUMMARY

In this paper we investigated the dynamics of a particle transfer between discrete states in two distant wells, separated by a reservoir with continuous spectrum. For this purpose we introduced continuous monitoring of the reservoir by an external observer (device), which registers a particle in the reservoir. An analysis of quantum motion under continuous observation can be performed by applying the quantum trajectory approach. In particular, we considered only the events where the particle never appears in the reservoir (null-result continuous

measurement). Quite unexpectedly, despite such a strict restriction, we found that the particle still appears in the second distant well, making its motion in the reservoir totally undetectable (we refer to this phenomenon as “teleportation”<sup>5</sup>).

Such a transition through the reservoir takes place through a *localized eigenstate* (bound state) embedded in the continuum. Although this state belongs to the continuum spectrum, its wave function is not extended into the reservoir and therefore is undetectable by monitoring the reservoir. Nevertheless it can mediate quantum transitions between distant wells.

In fact, the localized eigenstate embedded in continuum is analogous to a “dark” state in atomic system. The difference is that our state represents linear superposition of two components, largely separated in space. It becomes an eigenstate embedded in the continuum spectrum due to cancelation between different components of the eigenfunction in the continuum, thus revealing distracting quantum interference effect on large scales.

One expects, however, that the quantum interference would be destroyed if the motion of quantum particle is continuously monitored by an outside observer. A well-known example is an observation of quantum motion of a single particle in two slit experiment. This argument could imply that the quantum transfer through continuum between two isolated states would be destroyed either, whenever the particle’s motion in the reservoir is continuously observed. In particular, one anticipates that the continuous null-result measurement that never register the particle in the reservoir, prevents its transfer through continuum between distant wells. The above argument makes our results presented in this paper even more surprising, since the particle still penetrates through the reservoir, even it is *not* registered in it.

We demonstrated that the predicted teleportation phenomenon can be observed in different systems using the available technology. As an example we discussed a possible transfer of a single photon between distant cavities separated by a vacuum. Continuous non-invasive monitoring of the photon can be provided by the Kerr medium devices.

#### Acknowledgments

Two of us (X.Q.Li and S.G.) acknowledge to G. Huang for stimulating discussions. One of us (S.G.) acknowledges the Department of Physics, Beijing Normal University, and the State Key Laboratory for Superlattices and Microstructures, Institute of Semiconductors, Chinese Academy of Sciences for supporting his visit. Meanwhile, X.Q.Li acknowledges the Department of Chemistry, Hong Kong University of Science and Technology for supporting his visit. This work was supported by the NNSF of China under grants No. 101202101 & 10874176, and the Major State Basic Research Project.

- 
- <sup>1</sup> S.A. Gurvitz, Phys. Rev. B **57**, 6602 (1998).
- <sup>2</sup> J. Ping, X.Q. Li and S. Gurvitz, Phys. Rev. **A83**, 042112 (2011).
- <sup>3</sup> N. Katz *et al*, Science **312**, 1498 (2006).
- <sup>4</sup> B. Misra and E.C.G. Sudarshan, J. Math. Phys. **18** (1977).
- <sup>5</sup> The term “teleportation” is used here in its direct meaning, as a transfer of matter between two places without having to traverse the distance between them by conventional means. We distinguish it from the “quantum teleportation”, used in the literature. The latter is related to transfer of quantum information, but not the system itself<sup>6</sup>.
- <sup>6</sup> C.H. Bennett *et al*, Phys. Rev. Lett. **70**, 1895 (1993).
- <sup>7</sup> S.A. Gurvitz, Phys. Rev. **B77**, 201302(R) (2008).
- <sup>8</sup> J. von Neumann and E. Wigner, Z. Phys. **30**, 465 (1929);
- <sup>9</sup> H.M. Wiseman and G.J. Milburn, *Quantum Measurement and Control* (Cambridge University Press, Cambridge, 2010).
- <sup>10</sup> M.B. Plenio and S.F. Huelga, Phys. Rev. Lett. **88**, 197901 (2002); X.X. Yi, C.S. Yu, L. Zhou, and H.S. Song, Phys. Rev. **A68**, 052304, (2003).
- <sup>11</sup> W. Nagourney *et al*, Phys. Rev. Lett. **56**, 2797 (1986); J.C. Bergquist *et al*, *ibid.* **56**, 1699 (1986); Th. Sauter *et al*, *ibid.* **56**, 1696 (1986).
- <sup>12</sup> H.A. Bachor and T.C. Ralph, *A guide to experiments in quantum optics* (Wiley-VCH, 2004), 2nd ed.
- <sup>13</sup> Q.A. Turchette, C.J. Hood, W. Lange, H. Mabuchi, and H.J. Kimble, Phys. Rev. Lett. **75**, 4710 (1995).